Proceedings of Ninth World Conference on Earthquake Engineering
August 2-9, 1988, Tokyo-Kyoto, JAPAN (Vol.VIII)

SC-9

EARTHQUAKE RESPONSE ANALYSIS CONSIDERING SOIL-STRUCTURE SEPARATION USING CONTACT ELEMENTS AND DYNAMIC FLEXIBILITY OF SOIL IN TIME DOMAIN

Yasuhiro HAYASHI*, Nobuo FUKUWA*,
Shoichi NAKAI* and Yoshio KOYANAGI*

* Ohsaki Research Institute, Shimizu Corporation

SUMMARY

This paper presents a method of analysis which can consider the effects of soil-structure interaction including the local effects by soil-structure separation. The proposed method is based on a hybrid approach of finite element method in the time domain and boundary element method in the frequency domain. The soil-structure separation is represented by the contact element where the compatibility of internal forces and relative displacements between the nodes of soil and structure elements is satisfied. As an example, the dynamic characteristics of a nuclear reactor building subjected to vertically incident waves are studied using this method.

INTRODUCTION

The partial separation between soils and structures is recognized as an important phenomenon as well as soil-structure interaction, especially for the design and analysis of nuclear facilities. Finite element method is one of the most powerful approaches to evaluate the local behavior like soil-structure separation and the irregularity around the structure like backfill soils. When the nonlinearity and irregularity of the ground are limited near the structure, we sometimes apply the substructure technique combined with finite element method considering its computational efficiency. The substructure technique based on a flexibility formulation in the time domain, which takes into account linear unbounded soils, has been proposed by Wolf et al.(Ref. 1). This formulation involves the convolution integral of interaction forces and dynamic flexibility coefficients. The coefficients are not formulated in the time domain but are calculated as the inverse Fourier transform of the corresponding value in the frequency domain for the sake of simplicity in the formulation. But it may cause a divergence of the solution because of the effects of high frequency contents when the numerical transform using the FFT algorithm is applied. We present a substructure technique based on the flexibility formulation in the time domain. This formulation is similar to that by Wolf et al., but it depends upon the FFT algorithm and has the advantage in computational stability and efficiency.

Toki et al.(Ref. 2) have studied the separation and sliding between soil and structure using the joint element. The joint element can be regarded as a rigid spring which does not carry a tensile force and permits the sliding between the nodes of soil and structure elements. The accuracy of solution depends upon the stiffness of the joint element. On the other hand, the contact element is frequently used in contact problems under large deformations (Ref.3). In this paper, the soil-structure separation is represented by the contact element assuming infinitesimal

deformations. The contact element is equivalent to the joint element when the stiffness of the joint element approaches to infinity, i.e., the compatibility condition between the soil-structure interface is strictly satisfied.

METHOD OF ANALYSIS

The method of analysis is illustrated in Fig. 1. A reactor building and its irregular surrounding soil are discretized by finite elements. The soil-structure separation is evaluated by the contact elements and the soil far from the structure is represented by the flexibility formulation.

Flexibility Formulation We introduce the substructure concept into the soil-structure system as shown in Fig. 1. The entire soil-structure system can be partitioned into a set of much simpler two subsystems at an artificial boundary, the structure and near field subsystem and the far field subsystem. The equation of motion for the structure and near field subsystem is given by

$$\begin{bmatrix} \mathbf{M}_{SS} & \mathbf{M}_{SB} \\ \mathbf{M}_{BS} & \mathbf{M}_{BB} \end{bmatrix} \begin{Bmatrix} \ddot{\mathbf{u}}_S(t) \\ \ddot{\mathbf{u}}_B(t) \end{Bmatrix} + \begin{bmatrix} \mathbf{C}_{SS} & \mathbf{C}_{SB} \\ \mathbf{C}_{BS} & \mathbf{C}_{BB} \end{bmatrix} \begin{Bmatrix} \dot{\mathbf{u}}_S(t) \\ \dot{\mathbf{u}}_B(t) \end{Bmatrix} + \begin{bmatrix} \mathbf{K}_{SS} & \mathbf{K}_{SB} \\ \mathbf{K}_{BS} & \mathbf{K}_{BB} \end{bmatrix} \begin{Bmatrix} \mathbf{u}_S(t) \\ \mathbf{u}_B(t) \end{Bmatrix} = \begin{Bmatrix} \mathbf{0} \\ \mathbf{r}(t) \end{Bmatrix} \tag{1}$$

where $\mathbf{M}$, $\mathbf{C}$ and $\mathbf{K}$ are the mass, damping and stiffness matrices, $\mathbf{u}$ is displacement vector. Subscript B represents the degrees-of-freedom along the artificial boundary and S stands for the rest of them. The $\mathbf{r}(t)$ is the so-called interaction force vector due to incident seismic waves. The relationship between the motion of the boundary relative to the response $\dot{\mathbf{u}}_B{}^G(t)$ of the excavated far field and the boundary flexibility matrix $\dot{\mathbf{F}}(t)$ of the far field can be expressed in the frequency domain as $i\omega(\mathbf{u}_B(\omega)-\mathbf{u}_B{}^G(\omega))=i\omega\mathbf{F}(\omega)\cdot\mathbf{r}(\omega)$. Assuming a piecewise linear variation of the interaction force over every time step $((i\text{-}1)\Delta t<t<i\Delta t)$ and $(\dot{\mathbf{u}}_{Bn}+\dot{\mathbf{u}}_{Bn-1})\Delta t/2=\mathbf{u}_{Bn}-\mathbf{u}_{Bn-1}$, the interaction force at time t $(=n\Delta t)$ becomes

$$\mathbf{r}_n=\dot{\mathbf{F}}_0{}^{-1}\left[\frac{2}{\Delta t}(\mathbf{u}_{Bn}-\mathbf{u}_{Bn-1})-\dot{\mathbf{u}}_{Bn-1}-\dot{\mathbf{u}}_{Bn}^G-\sum_{i=1}^{l}\dot{\mathbf{F}}_i\,\mathbf{r}_{n-i}\right]$$

$$\dot{\mathbf{F}}_i=\int_0^{\Delta t}\frac{\tau'}{\Delta t}\dot{\mathbf{F}}((i+1)\Delta t-\tau')\,d\tau+\int_0^{\Delta t}\left(1-\frac{\tau'}{\Delta t}\right)\dot{\mathbf{F}}(i\Delta t-\tau')\,d\tau \tag{2}$$

The salient feature of this method is using $\dot{\mathbf{F}}(t)$, which consists of the impulse velocity responses, instead of using $\mathbf{F}(t)$ as Wolf(Ref. 1) did. In case of using $\mathbf{F}(t)$, it may cause a divergence of the solution because of the effects of high frequency contents, when $\mathbf{F}(t)$ is 0 at $t=0$, i.e. $\mathbf{F}_0\simeq\mathbf{0}$, and the numerical transform using the FFT algorithm is applied. But $\dot{\mathbf{F}}_0$ in Eq.(2) is so large compared with $\dot{\mathbf{F}}_n(n>0)$ that the solution is stable and accurate. It is also pointed out that l in Eq.(2) can be determined from the duration time of the impulse velocity responses which are much shorter than that of the earthquake ground motion. It is very efficient that small l leads to a reduction in the number of operations in evaluating the convolution integral. Furthermore, $\dot{\mathbf{F}}(t)$ is calculated only by the imaginary part of numerically obtained flexibility matrix $\mathbf{F}(\omega)$ considering the causality and reality of $\dot{\mathbf{F}}(t)$:

$$\dot{\mathbf{F}}(t) = F^{-1}(i\omega\mathbf{F}(\omega))+\mathbf{C} \simeq 2H(t)\cdot F^{-1}(-\omega\cdot\mathrm{Imag.}(\mathbf{F}(\omega))\cdot P_{\omega_c}(\omega))+\mathbf{C} \tag{3}$$

In Eq.(3), F^{-1} means the inverse Fourier transform and

$$H(t)=\begin{cases}0 & (t<0)\\ 1 & (t\geqq 0)\end{cases},\qquad P_{\omega c}(\omega)=\begin{cases}1 & (|\omega|<\omega_c)\\ 0 & (|\omega|\geqq\omega_c)\end{cases} \tag{4}$$

with $H(t)$ being a step function and $P_{\omega_c}(\omega)$ a low pass filter. Cut off frequency ω_c should be selected large enough. In order to make $\dot{\mathbf{F}}(t)$ tend to 0 as t increases, $\mathbf{C}$ can be determined in the time domain by the base line corrections. Hence we need not evaluate the static component of $\mathbf{F}(\omega)$ in Eq.(3).

Contact Element According to the condition of sticking, sliding and separating as shown in Fig.3., the contact element satisfies the compatibility condition of internal force **p** and relative displacement **δ** between the nodes of soil and structure finite elements. The equation of equilibrium is solved together with the compatibility condition as

$$\left(\begin{bmatrix} \mathbf{K} & 0 \\ 0 & 0 \end{bmatrix} + \begin{bmatrix} 0 & \mathbf{A}_{21}^{T} \\ \mathbf{A}_{21} & 0 \end{bmatrix} \right) \begin{Bmatrix} \mathbf{u} \\ \mathbf{p} \end{Bmatrix} = \begin{Bmatrix} \mathbf{q} \\ \boldsymbol{\delta} \end{Bmatrix} \tag{5}$$

in which **K**, **u** and **q** are the dynamic stiffness matrix, the displacement vector and the dynamic external force. $\mathbf{A}_{21}$ is the transformation matrix from the global coordinate to the local coordinate. Although the number of compatibility equations varies at each time step, the forward elimination of matrix **K** is needed only once by the arrangement of matrices and the assumption of infinitesimal deformations. The **u** and **p** are solved as

$$\mathbf{p} = \mathbf{K}_C^{-1}\left(\mathbf{A}_{21}\mathbf{K}^{-1}\mathbf{q} - \boldsymbol{\delta}\right) \quad , \quad \mathbf{u} = \mathbf{K}^{-1}\left(-\mathbf{A}_{21}^{T}\mathbf{p} + \mathbf{q}\right) \tag{6}$$

where

$$\mathbf{K}_C = \mathbf{A}_{21}\,\mathbf{K}^{-1}\mathbf{A}_{21}^{T} \tag{7}$$

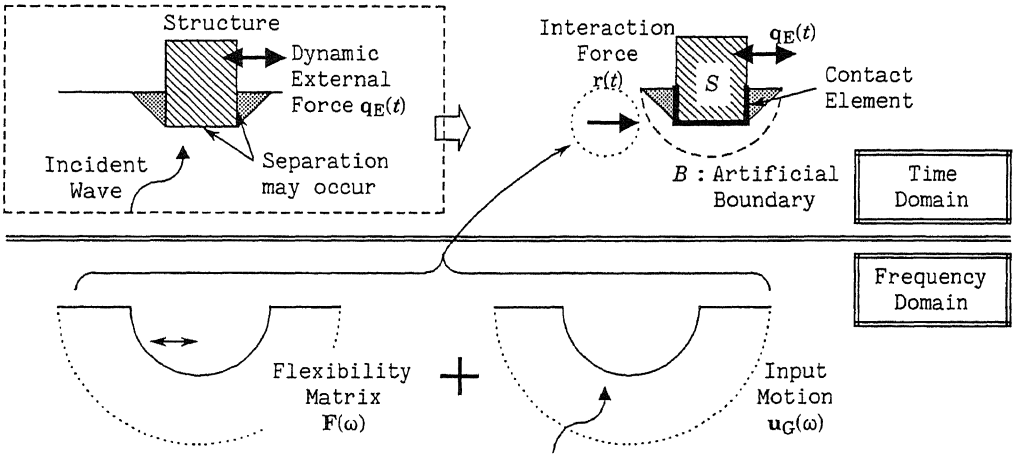

Fig.1 Schematic view of analysis and concept of substructure method

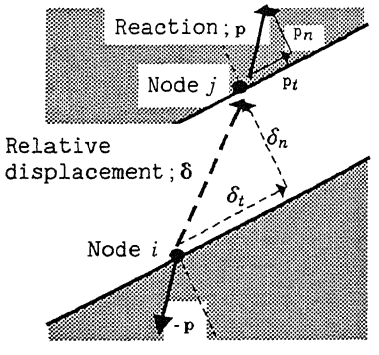

< Condition >			
Sticking	:	$\delta_n=0$, $\delta_t=0$,	$\lvert p_t\rvert<p_y$, $p_n<0$
Sliding	:	$\delta_n=0$, $\lvert\delta_t\rvert>0$,	$\lvert p_t\rvert=p_y$, $p_n<0$
Separating	:	$\delta_n>0$,	$p_t=0$, $p_n=0$

p_y : Yield shear force

Fig. 2 Compatibility condition of contact element

$\mathbf{K_C}$ is directly obtained by $\mathbf{K_C}^*$, which is calculated by substituting the transformation matrix $\mathbf{A_{21}}$ under the full sticking contact condition to Eq. (7) at the beginning of response analysis.

NUMERICAL RESULTS AND DISCUSSION

The effects of the separation between the side wall and ground is investigated using the prescribed method. An embedded BWR MARK II type reactor building as shown in Fig. 3 is adopted as an analysis model. Two soil models are chosen, one is homogeneous one and another includes backfill soil. The building and its surrounding soil are discretized by finite elements. The artificial ground motion depicted in Fig. 4 is considered as a vertically incident wave.

$\mathbf{F}(\omega)$ in Eq.(3) is calculated using the approximate three-dimensional boundary element method in the frequency domain (Ref. 4). Figure 5 shows the horizontal, rotational and vertical impedance functions when the artificial boundary is assumed to be rigid. Two results are plotted in the figure. The solid line corresponds to the original flexibility matrix $\mathbf{F}(\omega)$ and the dash line corresponds to the modified flexibility matrix $\tilde{\mathbf{F}}(\omega)$, which is due to the impulse velocity responses $\dot{\mathbf{F}}(t)$ obtained by Eq.(3) ($\omega_c/2\pi$=80Hz). These results are shown in their non-dimensional forms by using the shear modulus G, the half-width B(=64m) of excavated region and the half-depth L(=40m). The a_0 is the non-dimensional frequency, i.e., $a_0 = \omega L/V_s$, assuming V_s

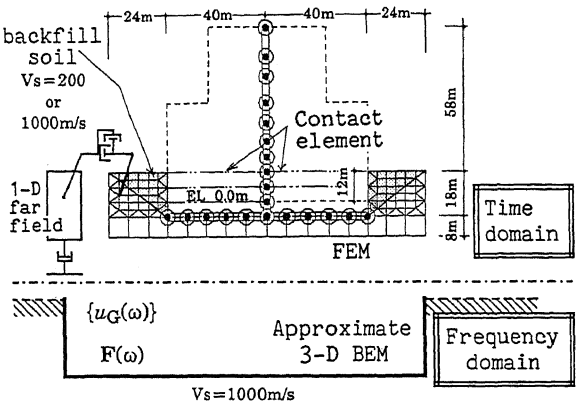

Fig.3 Description of analysis

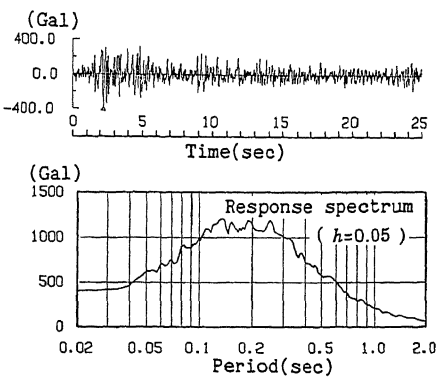

Fig.4 Artificial ground motion

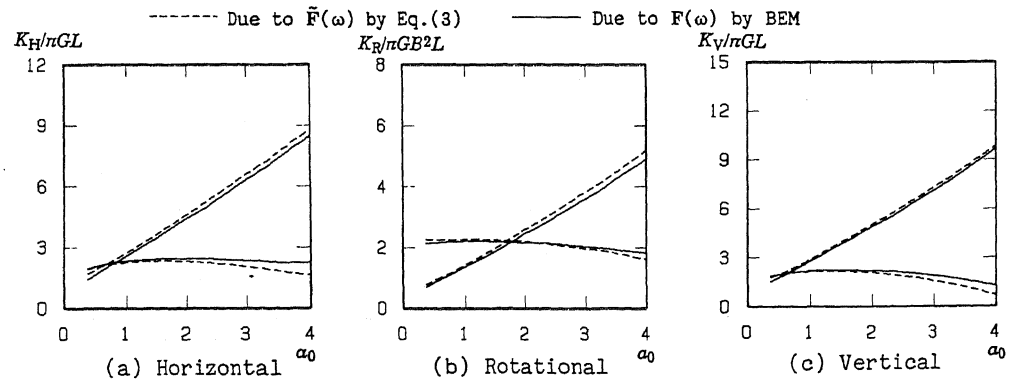

Fig.5 Impedance functions of artificial boundary

the shear wave velocity (=1000m/s). These results exhibit a fairly good agreement and the formulation in Eq. (3) is proved to be appropriate.

The soil pressure along the side wall is shown in Fig. 6. Figure 7 shows the time history of side wall-ground separation by the nonlinear response analysis. The upper line indicates to what level the separation goes at the right side wall, and the lower line at the left side wall. The maximum dynamic soil pressure of the homogeneous soil model (without backfill) is far greater than that with backfill. Since the backfill soil is much softer than surrounding soil, the backfill soil scarcely transmits the force between the soil and structure. However no much difference is observed in the static soil pressure of these two models. The separation occurs at the depth where the dynamic soil pressure cancels the initial soil pressure. As a result, the separation occurs in the homogeneous soil model more widely and frequently than in the model with backfill.

The maximum response values by the linear and nonlinear analyses are shown in Fig. 8. The maximum acceleration and shear force values of the model with backfill are hardly affected by the separation. For the homogeneous soil model, however, the maximum response values by nonlinear analysis decrease above the ground level and increase below the ground level compared with that by linear analysis. It is also mentioned that, if the nonlinear effect is considered, the maximum response of the homogeneous soil model approaches that of the model with backfill. It seems that the effect of separation is equivalent to the reduction in the soil stiffness around the side wall. Figure 9 indicates the floor response spectra. The tendency of variation due to the separation correspond to that of maximum response value in acceleration.

CONCLUSIONS

The method of earthquake response analysis considering soil-structure separation using the contact element and flexibility formulation is presented. The flexibility formulation is practically very useful as well as numerically efficient and stable. Since $\dot{F}(t)$ in Eq.(3) is determined without the static component of dynamic flexibility coefficients $F(\omega)$ in the frequency domain, $F(\omega)$ can be obtained by various methods like the boundary element analysis or the finite element analysis with the energy transmitting boundary and viscous boundary.

The method was applied to an embedded reactor building in order to investigate the effects of separation between the soil and side wall. The effects of the side wall-ground separation are found to be strongly affected by the soil condition around the side wall and it may cause the reduction of the embedment effects.

ACKNOWLEDGMENT

The authors wish to express their gratitude to Dr. Y. Katsukura of Ohsaki Research Institute for his valuable suggestion.

REFERENCES

1) Wolf, J. P. et al., "Non-linear Soil-structure-interaction Analysis Using Dynamic Stiffness or Flexibility of Soil in the Time Domain", J. of E.E. & S.D., pp. 195-212, 1985
2) Bathe, K. J. et al.,"A Solution Method for Planar and Axisymmetric Contact Problems ", Int. J. Num. Meth. in Eng., pp. 65-88, 1985
3) Toki, K. et al., "Separation and Sliding between Soil and Structure during Strong Ground Motion", J. of E.E. & S.D., pp. 263-277, 1981
4) Nakai, S. et al., "Approximate three dimensional analyses of embedded structures", Proc. of 8th WCEE., 1984

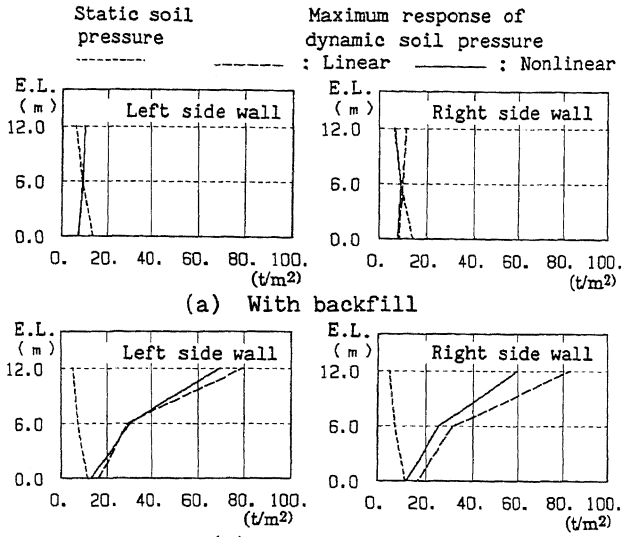

(a) With backfill

(b) Homogeneous

Fig.6 Soil pressure

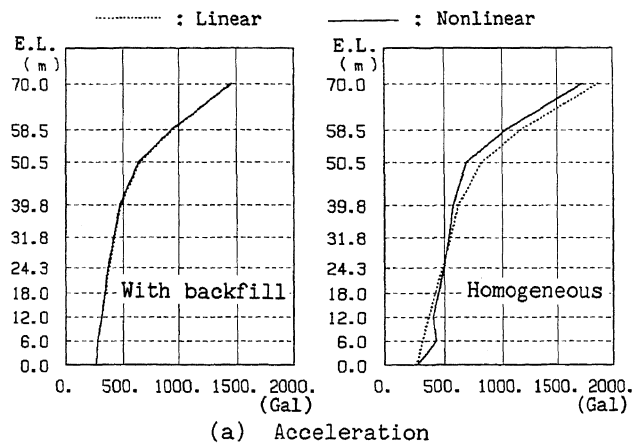

(a) Acceleration

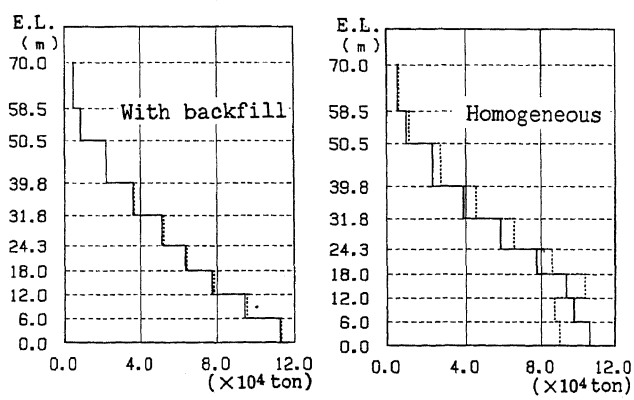

(b) Shear force

Fig.8 Maximum response

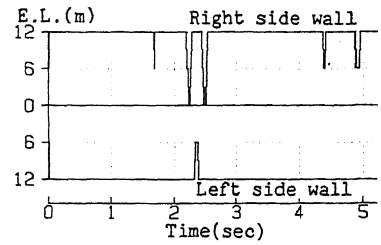

(a) With backfill

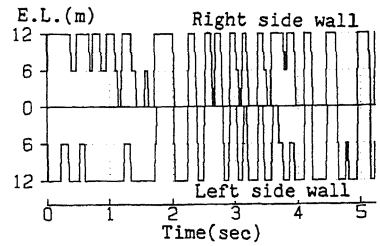

(b) Homogeneous

Fig.7 Time history of side wall-ground separation

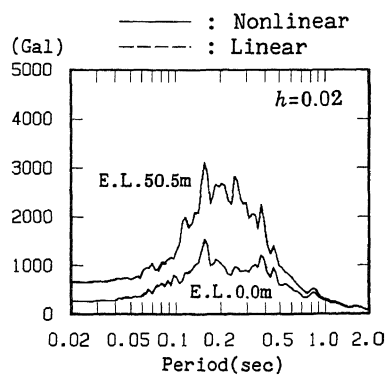

(a) With backfill

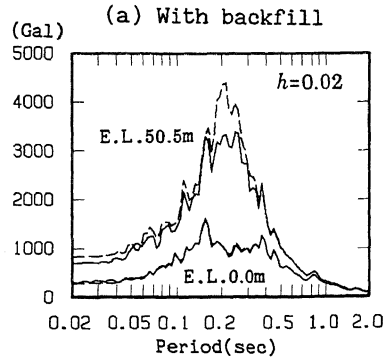

(b) Homogeneous

Fig.9 Response spectra